Regeneration of manganese oxide as adsorption sites for hydrogen sulfide on granulated coal ash

Asaoka, Satoshi ; Okamura, Hideo ; Akita, Yusuke ; Nakano, Katsuyoshi ; Nakamoto, Kenji ; Hino, Kazutoshi ; Saito, Tadashi ; Hayakawa, Shinjir…

(Citation)
Chemical Engineering Journal,254:531-537

(Issue Date)
2014-10-15

(Resource Type)
journal article

(Version)
Accepted Manuscript

Regeneration of manganese oxide as adsorption sites for hydrogen sulfide on granulated coal ash

Satoshi ASAOKA[a*], Hideo OKAMURA[a], Yusuke AKITA[b], Katsuyoshi NAKANO[b], Kenji NAKAMOTO[c], Kazutoshi HINO[c], Tadashi SAITO[c], Shinjiro HAYAKAWA[d], Misaki KATAYAMA[e], Yasuhiro INADA[e]

[a] Research Center for Inland Seas, Kobe University
5-1-1 Fukaeminami, Higashinada, Kobe, 658-0022 JAPAN

[b] Faculty of Maritime Sciences, Kobe University
5-1-1 Fukaeminami, Higashinada, Kobe, 658-0022 JAPAN

[c] The Chugoku Electric Power Co., Inc.
4-33, Komachi,Naka-ku,Hiroshima-shi,Hiroshima, 730-8701 JAPAN

[d] Graduate School of Engineering, Hiroshima University
1-4-1 Kagamiyama, Higashi-Hiroshima, Hiroshima 739-8527, Japan

[e] College of Life Science, Department of Applied Chemistry, Ritsumeikan University
1-1-1 Nojihigashi Kusatsu, Shiga 525-8577, Japan

*Corresponding author:

Tel & Fax: +81-78-431-6357, E-mail: s-asaoka@maritime.kobe-u.ac.jp

Address: Research Center for Inland Seas, Kobe University, 5-1-1 Fukaeminami, Higashinada, Kobe, 658-0022 JAPAN

Abstract

It is important to remove hydrogen sulfide to maintain healthy ecosystems as well as viable aquaculture activities in enclosed water bodies. Granulated coal ash with high adsorption capacity for hydrogen sulfide is a by-product generated from coal combustion processes in coal-fired power plants. The purposes of this study were to (1) verify the regeneration of the adsorption sites for hydrogen sulfide on the granulated coal ash by redox reaction which changes between oxic and anoxic conditions and (2) prove the regeneration mechanisms of the adsorption site which leads to high adsorption capacity for hydrogen sulfide. XAFS analyses of the granulated coal ash revealed that the adsorption site for hydrogen sulfide on the granulated coal ash was regenerated at least 10 times through oxidation of manganese oxide under oxic conditions. A positive correlation (r=0.995) between the peak top energy of manganese XAFS in the GCA collected from field trial sites and the Eh of the sediments applied with the GCA was observed. These results proved that hydrogen sulfide was adsorbed and oxidized by the granulated coal ash during the stratified season. During the vertical mixing seasons, oxygen regenerates the adsorption site for hydrogen sulfide. It is concluded that this regeneration of adsorption site gives the granulated coal ash high adsorption capacity for hydrogen sulfide.

Key words

Coal-fired power plant, Eutrophication, Manganese oxide, Recycled materials, Sulfur, XAFS

1. Introduction

Eutrophication is one of the most serious environmental problems in enclosed water bodies. The excessive terrigenous nutrient loads as well as nutrient dissolution from eutrophic sediments lead to massive growth of algae. As a result, hypoxic water is induced due to the decomposition of the dead cells in stratified seasons. Under such anoxic condition, hydrogen sulfide is produced through the reduction of sulfate ions by sulfate-reducing bacteria. Hydrogen sulfide is harmful for living organisms, and also consumes oxygen when it is oxidized. It exerts a negative impact on aquatic organisms even at low concentrations of 0.1 to 2 mg L^{-1}, because it interferes with cytochrome c oxidase, the last enzyme of the electron transport system [1, 2]. However, a high level of hydrogen sulfide is observed in eutrophic marine sediment pore water throughout the world [3-6]. Therefore it is very important to reduce the hydrogen sulfide concentration in eutrophic sediments so as to maintain healthy ecosystems and aquaculture activities.

Granulated coal ash (GCA) is a by-product generated from coal combustion processes in coal-fired power plants. Previous studies have proven that GCA adsorbed effectively hydrogen sulfide. The removal mechanism of hydrogen sulfide was possible through oxidation by manganese oxide on the GCA [7]. The GCA has a high adsorption capacity [8] of 108 mg S g^{-1} for hydrogen sulfide compared to other materials such as 37.5-S mg g^{-1} for noncarbonated steel slag [9], and 12 mg-S g^{-1} for crushed oyster shells [10], 2.3-71 mg-S g^{-1} for activated carbons [11, 12]. Furthermore, the GCA applied into the sediment in enclosed water bodies at a field experiment site has suppressed hydrogen sulfide for over 5 years. On the other hand, it has been demonstrated that conventional methods such as sand coverage could suppress hydrogen sulfide for a few years. Given that the GCA has such a high adsorption capacity for hydrogen sulfide, this long term suppression observed in the field experiment site might be considered as regeneration of the adsorption sites for hydrogen sulfide under natural conditions which change between oxic to anoxic conditions annually. During the stratified seasons (summer), the bottom layer of the water column in eutrophic enclosed water bodies is in a reduced, or anoxic condition due to the consumption of dissolved oxygen through the decomposition of organic matter. When moving into the vertical mixing seasons (spring and autumn), oxygen is introduced into the bottom of the water column with vertical mixing and hypoxic water disappears. We then developed a hypothesis as follows: The GCA on the manganese oxide oxidizes hydrogen sulfide with coupling reduction of manganese oxide under reduced condition. The reduced manganese oxide on the GCA might be oxidized again, in other words, regenerated by dissolved oxygen during the vertical mixing seasons.

The purpose of this study was to reveal the regeneration of the adsorption sites by proving redox reaction on the surface of the granulated coal ash using XAFS.

2. Materials and methods

2.1 Granulated coal ash

The GCA with 5 mm diameter tested in this study is produced through the granulation process of coal fly ash from coal used in thermal electric power stations (Chugoku Electric Power) with added cement as binder amounting to approximately 15% of the final product. It is mainly composed of SiO_2, CO_3, Al_2O_3, CaO, organic carbon, and Fe_2O_3 with quartz and aluminosilicate crystal phase, and their concentrations are 395, 133, 126, 55.4, 27.4, and 22.5 g kg^{-1}, respectively. TiO_2 and MnO contents are 5.68 g kg^{-1} and 329 mg kg^{-1}, respectively [7]. The environmentally regulated substances dissolved from the GCA used in this study were obviously below the standard levels for environmental criteria in Japan [13].

2.2 Removal experiments for hydrogen sulfide

The hydrogen sulfide solution was prepared as follows: Tris-HCl buffer (Kanto Kagaku) was diluted with ultrapure water to prepare 30 mmol L^{-1} of buffer solution (pH=8.2). The buffer solution was deaerated with N_2 gas. Successively, an aliquot of $Na_2S \cdot 9H_2O$ (Wako Pure Chemical Industries) was dissolved to make a 10 or 100 mg-S L^{-1} hydrogen sulfide solution representing the possible range in the pore water of organically enriched sediments. The batch experiments were conducted in triplicate. Fifty mL of the hydrogen sulfide solution was slowly dispensed into a 100 mL DO bottle, and 0.2 g of the GCA was added to the hydrogen sulfide solution. Thereafter, the head space of the bottle was replaced with N_2 gas and capped tightly using grease for vacuum use. In the case of samples treated with an initial concentration of 10 mg-S L^{-1}, the 100 mL vial bottles sealable by a rubber cork with an aluminum cap were used instead of the DO bottles in order to improve sealed conditions. Thereafter, it was agitated moderately at 100 rpm at 25°C in a constant-temperature oven for 24 h under anoxic condition. The time courses of hydrogen sulfide concentration were measured using a detection tube (200SA or 200SB: Komyo Rikagaku Kougyo). The detection tube can measure aqueous hydrogen sulfide concentration in sulfur equivalent with forming a brown color band length. After 24 h, the hydrogen sulfide solution was replaced by 50 mL of 30 mmol L^{-1} Tris-HCl buffer solution (pH 8.2) and the cap of the bottle was also replaced by a silicon plug to allow exchange of gases. Thereafter, it was agitated moderately at 100 rpm at 25°C in the constant-temperature oven for 24 h under oxic condition. After 24 h, the Tris-HCl buffer solution was replaced again by 50 mL of hydrogen sulfide solution described above. This removal experiments for hydrogen sulfide were continued repeatedly following the steps in Fig. 1. Control experiments were also carried out without the GCA. The amount of removal sulfur, X (mg g^{-1}) with the GCA was calculated followed by equation (1).

$$X = \frac{(C_b - C_g) * V}{G} \quad \cdot \cdot \cdot (1)$$

Where, X, C_b, C_g, V and G were the amount of removal sulfur (mg g^{-1}), the concentration of hydrogen sulfide at time t in the blank (mg L^{-1}), the concentration of hydrogen sulfide at time t in the GCA bottle (mg L^{-1}), liquid phase volume (0.05 L) and the amount of the GCA (0.2 g).

The precipitation observed in this removal experiments was collected by filtering through a membrane filter (Omnipore: Millipore) with a pore size of 0.45 μm. The precipitate was dried in a nitrogen gas atmosphere and thereafter kept in a vacuum-sealed packing before XAFS analyses.

In order to quantify sulfate and thiosulfate ion desorbed from the GCA under oxic conditions, sulfate and sulfate ion in the solution was measured by an ion chromatograph (ELITE LaChrom : HITACHI) attached with an anion column (#2470; 4.6 mm ϕ ×150 mm :HITACHI) and a conductivity detector (L-2470 : HITACHI). The solution was beforehand filtered through a 0.45 μm syringe filter (Millex: Millipore) and diluted 10 times with ultrapure water to prevent analytical interference of the Tris-HCl buffer solution.

The GCA reacted with 100 mg L^{-1} of the initial hydrogen sulfide concentration was analyzed by XAFS as described below.

2.3 GCA sampling from field trials

The GCA distributed in the sea bottom sediments during the field trials was also collected. The latitude, longitude and environmental parameters of the each sampling station are shown in Fig. 2 and Table 1, respectively. All the sampling stations are located in Japan.

St. 1 --- Kyobashi-River is a tidal river flowing through Hiroshima city which is one of the big metropolis in Japan. The muddy sediments were observed in the river bottom because the river was affected by terrigenous load and salinity intrusion from Hiroshima Bay.

St.2 --- Onoda is located inside an enclosed port surrounded by industrial complexes. The sediment was affected by terrigeneous load from Onoda city and industrial wastewater.

St. 3 --- Kaita Bay is fringing the northern edges of Hiroshima Bay and receives river discharge from the Seno River [14]. Muddy sediment was also accumulated in Kaita Bay. High levels of hydrogen sulfide was observed in the muddy tidal flat formed along the Seno River bank [5].

St. 4 --- Nakaumi is an enclosed brackish lake inscribed as wetlands under the Ramsar Convention. However, Nakaumi was significantly affected by terrigeneous load from paddy fields and domestic water. Therefore, hypoxic water is observed every summer and the production of clams there decreased sharply in recent years.

St. 5 --- Tabuse is covered on four sides by small islands. The seawater exchange is topographically low. Therefore organically enriched sediment was accumulated therein.

The GCA applied on sediments was collected into a vial with seawater below the sea surface and the vial was capped tightly in the seawater by a diver at Stations 2 to 5. The GCA at St. 1 was collected into a vial with river water at 30 cm depth from a river bed and the vial was capped tightly. The sealed GCA samples were transported to a laboratory and kept in a cool and dark condition. After arriving at the laboratory, the GCA samples were dried in a nitrogen gas atmosphere and thereafter kept in a vacuum-sealed packing before XAFS analyses.

The dissolved oxygen (DO) and salinity of overlying waters were measured by a multi electrode (Quanta G: HYDROLAB). The pH and Eh of the sediment were also determined by a pH electrode (HM-20P: DKK-TOA) and an ORP electrode (RM-30P:DKK-TOA), respectively. The concentration of hydrogen sulfide in pore water was analyzed by gas chromatography [15].

2.4. X-ray absorption fine structure (XAFS) analyses and data processing

Sulfur K edge XAFS spectra (ranges 2460-2490 eV) were measured using the BL11 in the Hiroshima Synchrotron Research Center, HiSOR. The synchrotron radiation from a bending magnet was monochromatized with a Si(111) double-crystal monochromator. The sample chamber was filled with He gas, and XAFS spectra were measured both by the X-ray fluorescence yield (XFY) mode using a SDD detector (XR-100SDD; AMPTEK) and conversion electron yield (CEY) mode. The X-ray energy around K edges of sulfur was calibrated with the spectra of $CuSO_4$ obtained with the CEY mode. The K edge main peak of sulfate was set to 2481.6 eV [7]. The pieces of relatively flat GCA samples were mounted on a double-stick tape (NW-K15; Nichiban) placed in the central hole (15 mm in diameter) of a copper plate. The surface of the sample was attached to that of the copper plate. The angle between the incident X-ray and the sample surface was adjusted at 20 degrees, and the X-ray fluorescence was detected from the direction normal to the incident beam in the plane of electron orbit of the storage ring.

Manganese and iron K edge XAFS spectra (range 6500-6600 eV for manganese and range 7080-7200 eV for iron) were measured using BL3 at the Ritsumeikan SR Center, Japan. The synchrotron radiation was monochromatized with a Si(220) double-crystal monochromator. The sample XAFS spectra were measured by X-ray fluorescence yield mode using a three-elements Ge solid state detector, SSD (GUL0110S: Canberra). Samples were sealed with polypropylene film and they were positioned at 45 degrees to the incident beam in fluorescence mode. The X-ray energy was calibrated by defining the K edge pre-edge peak of d-MnO_2 and hematite obtained by the transmission mode to be fixed at 6540 and 7112 eV, respectively [7]. An ionization chamber for the transmission mode was filled with mixed gases: Ar 15% and N_2 85% for the incident chamber (Io) and Ar 50% and N_2 50% for the transmitted chamber (I). The spectra obtained by these XAFS analyses were processed with XAFS spectra processing software (REX2000 ver. 2.5: Rigaku co. Ltd.).

3. Results and Discussion

3.1 Removal experiments for hydrogen sulfide

Removal amount of hydrogen sulfide with time by the GCA at initial hydrogen sulfide concentration 10 and 100 mg-S L^{-1} were shown in Figs. 3a and 3b, respectively. The removal amount of hydrogen sulfide did not change in the number of removal tests. On the contrary, in the case with an initial concentration of 10 mg-S L^{-1}, the removal amount of hydrogen sulfide conducted 11 times (11th in Fig. 3a) was higher than that of the other removal tests (p: probability <0.01-0.05). When the initial concentration was 100 mg-S L^{-1}, the removal amount of hydrogen sulfide at 4 to 10 times (4th, 5th and 10th in Fig. 3b) was higher than that of 1 to 3 times ($p<0.01\sim0.05$) at 12 h. This increase was attributed to precipitation because a white colored precipitation was observed with increasing frequency of the test under anoxic condition. The formation of the white colored precipitation might have increased the removal amount of hydrogen sulfide.

The white colored precipitation observed in the 100 mg-S L^{-1} hydrogen sulfide adsorption experiments was submitted to XAFS analyses so as to identify sulfur species (Fig. 4). The sulfur K edge XAFS spectra of the white colored precipitation were quite similar to that of sulfur standard which has a peak of around 2472 eV. Thus, the white colored precipitation was identified as sulfur. On the other hand, the white colored precipitation was not observed under oxic condition, which was supported by the fact that the sulfur K edge XAFS spectra were not identified on the filter used under oxic condition.

The manganese K edge spectra of manganese oxide standards and the GCA are shown in Fig. 5. It is already known that hydrogen sulfide was adsorbed onto the GCA and successively oxidized by manganese oxide (III) contained in the GCA. The oxidation reaction of hydrogen sulfide was coupled with the reduction of manganese oxide [7]. The small pre-edge peaks in XANES are attributed to the 1s-3d transition, which is sensitive to the valence of manganese atoms [16]. However, the manganese concentration in the GCA was not high enough to obtain clear pre-edge peaks. Instead, peak top energy is also quite different between divalent and trivalent forms [7, 16, 17]. In this study, we discussed the redox reaction of manganese using peak top energy.

The GCA tested in this study initially has a peak top around 6555.7 eV. After 1 time hydrogen sulfide adsorption stage (H_2S 1st in Fig. 5), the peak top at 6555.7 eV shifted to around 6551.3 eV, indicating that the manganese oxide on the GCA was reduced by hydrogen sulfide. Thereafter the GCA was moved to oxic condition (oxic condition 1st time stage ; Oxic 1st in Fig. 5), the peak of around 6555.7 eV was identified again. However the peak around 6551.3 eV has not disappeared completely, indicating that the reduced manganese oxide in the GCA was partially oxidized under oxic condition. In other words, the partial oxidation of the reduced manganese oxide means partial regeneration of adsorption site for hydrogen sulfide.

Successively, the GCA was moved again to the anoxic condition. After 2 times hydrogen sulfide adsorption stage (H_2S 2nd in Fig, 5) the peak top of around 6555.7 eV shifted to 6551.3 eV coupling with the oxidation of hydrogen sulfide, indicating that the regenerated adsorption site could also adsorb and oxidize hydrogen sulfide.

Similarly, when the redox condition changed from anoxic to oxic, the peak top shift representing a redox reaction of manganese oxide on the GCA was observed repeatedly suggesting that the adsorption site for hydrogen sulfide could be regenerated at least 10 times.

In contrast, the peak top of iron K edge XAFS on the GCA has not shifted with changes in redox condition (Fig. 6). In other words, iron was not involved in the redox reaction. Therefore, the iron did not play an important role for hydrogen sulfide oxidation.

The sulfur K edge XAFS of sulfur standards and the GCA are shown in Fig. 7. The initial GCA had a peak top of around 2481.7 eV representing sulfate originating from cement and coal fly ash [18].

After adsorption of hydrogen sulfide (H_2S 1st to 10th in Fig. 7), the new peak was identified at around 2472 eV representing sulfur. The sulfur peak remained under oxic condition (oxic 1st to 10th in Fig. 7). The sulfate and thiosulfate ion which were formed through the oxidation of sulfur dissolved from the sulfur adsorbed GCA were quantified under oxic condition experiments. Sulfate and thiosulfate did not dissolve from the GCA, <0.04 mg g^{-1}, <0.1 mg g^{-1}, respectively, except at the oxic 1st stage. At the oxic 1st stage, 0.46 mg g^{-1} of sulfate was dissolved from the GCA. The sulfate was derived from cement and coal fly ash [18]. The sulfate dissolution was consistent with XAFS results. The sulfate peak of initial GCA disappeared through the removal experiments due to the dissolution of the sulfate.

Consequently, the adsorbed sulfur derived from oxidation of hydrogen sulfide by the manganese oxide on the GCA was stable under both anoxic and oxic conditions.

3.2. The XAFS analyses of GCA from field trials

The K edge manganese XAFS spectra of the GCA collected from field trial sites are shown in Fig. 8. The characteristics of the each sampling are also shown in Table 1. The GCA collected from St. 1 Kyobashi-River had the highest peak top energy of all the sampling stations. On the other hand, the GCA at St. 3 Kaita Bay had the lowest energy. Because the St. 1 Kyobashi-River becomes exposed at low tide periods, air can be introduced into the sediment. Therefore, the Eh of the sediment at St. 1 Kyobashi-River was 362 mV, which was the highest among all the sampling stations (Table 1). In other words, the sediment at St. 1 Kyobashi-River was in an oxic condition. Conversely, the Eh of the sediment at St. 3 Kaita Bay was lowest at -14.9 mV because it was enclosed and affected by significant terrigenous loads. The decomposition of organic matter with consuming dissolved oxygen was likely to decrease the sediment Eh. A positive correlation between the peak top energy of manganese XAFS in the GCA collected from field trial sites and the Eh of the sediments applied with the GCA was observed (Fig. 9). The oxidation state of manganese oxide in the GCA changed depending on the Eh of the sediments. This is because manganese species are redox dependent [19]. Consequently, the adsorption site for hydrogen sulfide on the GCA might be regenerated under oxic conditions in the real environment.

The sulfur peak at 2472 eV was also observed from the GCA collected from the field trial sites (Fig. 10). The sulfur peaks were relatively small because the sulfate originated from seawater which has a large peak at 2481.6 eV. Although the sulfur peaks were relatively small, it could be said that the hydrogen sulfide was oxidized to sulfur and remained stable on the GCA in the real environment. These manganese and sulfur XAFS results are consistent with results from removal experiments conducted in a laboratory.

3.3 Regeneration mechanisms of the adsorption site for hydrogen sulfide on the GCA and filed application

The regeneration mechanisms of the adsorption site for hydrogen sulfide on the GCA are shown in Fig. 11. (1) Hydrogen sulfide is adsorbed on the GCA and oxidized to sulfur coupling with manganese oxide reduction on the surface of the GCA under anoxic conditions or stratified season. (2) The sulfur adsorbed on the GCA partially separates from the GCA as a sulfur precipitation with increasing sulfur layer on the GCA. (3) When the redox condition moves to oxic or vertical mixing season, the manganese on the peeled surface of GCA was oxidized by oxygen. The regenerated adsorption site can adsorb and oxidize hydrogen sulfide. These processes are repeated every season. If anoxic condition is maintained for an extended period, the adsorption site for hydrogen sulfide might not be regenerated. As a result, the adsorption capacity might decrease with the coverage of the sulfur layer [8]. In contrast, in this study, the sulfur adsorbed on the GCA partially separated from the GCA as a sulfur precipitate with increasing sulfur layer on the GCA. The removed amount of hydrogen sulfide did not decrease under our experimental condition.

Based on the results obtained in this study, the application of the GCA to organically enriched sediments is effective in reducing hydrogen sulfide in sediment pore water for a long time. In our proposed method, the GCA is simply scattered or mixed with the organically enriched sediment accumulated in eutrophic areas such as enclosed water bodies, innermost areas of bay, lakes, and tidal rivers using a dredging boat to remove hydrogen sulfide [20-22]. Furthermore, laboratory and field trials in this study showed that the applied GCA in actual field sites need not be collected because the adsorption site for hydrogen sulfide on the GCA could be regenerated during the vertical mixing seasons. This simple remediation technology involving the scattering or mixing of the GCA with organically enriched sediments also holds much promise for environmental restoration in many developing countries where expensive remediation technology is generally impractical.

Conclusion

The adsorption site for hydrogen sulfide was regenerated through manganese oxidation at least 10 times under oxic conditions. This result proved that hydrogen sulfide was adsorbed and oxidized by the GCA during the stratified season. Moving into the vertical mixing seasons, oxygen regenerates the adsorption site for hydrogen sulfide on the GCA. These mechanisms give the GCA a high adsorption capacity for hydrogen sulfide in the field.

Acknowledgements

This study was partially supported by the Adaptable and Seamless Technology Transfer Program through Target-driven R & D (A-STEP), Feasibility study stage, AS242Z02839N provided by the Japan Science and

Technology Agency.

XAFS analyses at the SR Center, Ritsumeikan University, and the Hiroshima Synchrotron Radiation Center, Hiroshima University were partially carried out under the approval of Project for Creation of Research Platforms and Sharing of Advanced Research Infrastructure (R1225 and R1311) and the collaborative research (12-A-4), respectively.

This study was conducted under a joint research between Kobe University and The Chugoku Electric Power Co., Inc.

We are grateful to Dr. Keishi Nishihara and coordinator Norio Kawaguchi (Center for Collaborative Research and Technology Development, Kobe University) for their helpful comments about this research.

This manuscript was critically edited by a native English speaker, Dr. Lawrence M. Liao of the Graduate School of Biosphere Science at Hiroshima University.

References

[1] K. Marumo, M. Yokota, Review on aoshio and biological effects of hydrogen sulfide. Rep. Mar. Ecol. Res. Inst. 15 (2012) 23-40. in Japanese.

[2] E.G. Affonso, V. L. P. Polez, C. F. Corrêa, A. F. Mazon, M. R. R. Araújo, G. Moraes, F. T. Rantin, Physiological responses to sulfide toxicity by the

air-breathing catfish, *Hoplosternum littorale* (Siluriformes, Callichthyidae), Comparative Biochem. Physiol., C 139 (2004) 251-257.

[3] M. A. K. Azad, S. Ohira, M. Oda, K. Toda, On-site measurements of hydrogen sulfide and sulfur dioxide emissions from tidal flat sediments of Ariake Sea, Japan, Atmos. Environ. 39 (2005) 6077-6087.

[4]B. K. Reese, M. A. Anderson, C. Amrhein, Hydrogen sulfide production and volatilization in a polymictic eutrophic saline lake, Salton Sea, California, Sci. Total Environ. 406 (2008) 205-218

[5] T. Yamamoto, S. Kondo K. H. Kim, S. Asaoka, H. Yamamoto, M. Tokuoka, T. Hibino, Remediation of muddy tidal flat sediments using hot air-dried crushed oyster shells, Mar. Pollut. Bull. 64 (2012) 2428-2434.

[6] S. Asaoka, T. Yamamoto, Y. Takahashi, H. Yamamoto, K. H. Kim, K. Orimoto, Development of an on-site simplified determination method for hydrogen sulfide in marine sediment pore water using a shipboard ion electrode with consideration of hydrogen sulfide oxidation rate, Interdisciplinary Studies Environ. Chem. – Environ. Poll. Ecotoxicol. 6 (2012) 345-352.

[7] S. Asaoka, S. Hayakawa, K. H. Kim, K. Takeda, M. Katayama, T. Yamamoto, Combined adsorption and oxidation mechanisms of hydrogen sulfide on granulated coal ash, J. Colloid Interf. Sci. 377 (2012) 284-290.

[8] S. Asaoka, T. Yamamoto, S. Hayakawa, Removal of hydrogen sulfide using granulated coal ash, J. Jpn. Soc. Water Environ. 32 (2009) 363-368 (in Japanese with English abstract).

[9] K. H. Kim, S. Asaoka, T. Yamamoto, S. Hayakawa, K. Takeda, M. Katayama, T. Onoue, Mechanisms of hydrogen sulfide removal with steel making slag, Environ. Sci. Technol. 46 (2012) 10169-10174.

[10] S. Asaoka, T. Yamamoto, S. Kondo, S. Hayakawa, Removal of hydrogen sulfide using crushed oyster shell from pore water to remediate organically enriched coastal marine sediments, Biores. Technol. 100 (2009) 4127-4132.

[11] J. Guo, Y. Luo, A. C. Lua, R. Chi, Y. Chen, X. Bao, S. Xiang, Adsorption of hydrogen sulphide (H_2S) by activated carbons derived from oil-palm shell, Carbon 45 (2007) 330-336.

[12] Y. Xiao, S. Wang, D. Wu, Q. Yuan, Experimental and simulation study of

hydrogen sulfide adsorption on impregnated activated carbon under anaerobic conditions, J. Hazard. Mater. 153 (2008) 1193-1200.

[13] S. Asaoka, T. Yamamoto, K. Yamamoto, A preliminary study of coastal sediment amendment with granulated coal ash-Nutrient elution test and experiment on *Skeletonema costatuum* growth- , J. Jpn. Soc. Water Environ. 31 (2008)455-462. (in Japanese with English abstract)

[14] S. Asaoka, T. Yamamoto, Phosphorus mass balance in a highly eutrophic semi-enclosed inlet near a big metropolis: A small inlet can contribute towards particulate organic matter production, Mar. Pollut. Bull. 63 (2011) 237-242.

[15]G. A. Cutter, T. J. Oatts, Determination of dissolved sulfide and sedimentary sulfur speciation using gas chromatography-photoionization detection, Anal. Chem. 59 (1987)717-721.

[16] Y. Zhang, Z. Qin, G. Wang, H. Zhu, M. Dong, S. Li, Z. Wu, Z. Li, Z. Wu, J. Zhang, T. Hu, W. Fan, J. Wang, Catalytic performance of MnOx–NiO composite oxide in lean methane combustion at low temperature, Appl. Catal. B 129 (2013)172-181.

[17] S. Asaoka, H. Okamura, R. Morisawa, H. Murakami, K. Fukushi, T. Okajima, M. Katayama, Y. Inada C. Yogi, T.Ohta, Removal of hydrogen sulfide using carbonated steel slag, Chem. Eng. J. 228 (2013) 843-849.

[18] A. Jaworek, T. Czech, A. T. Sobczyk, A. Krupa, Properties of biomass vs. coal fly ashes deposited in electrostatic precipitator, J. Electrostat. 71 (2013)165-175.

[19] C. Lenz, T. Behrends, T. Jilbert, M. Silveira, C. P. Slomp, Redox-dependent changes in manganese speciation in Baltic Sea sediments from the Holocene Thermal Maximum: an EXAFS, XANES and LA-ICP-MS study, Chem. Geol. 370(2014)49-57.

[20] K. H. Kim, T. Hibino, T. Yamamoto, S, Hayakawa, Y. Mito, K. Nakamoto, I. C. Lee, Field experiments on remediation of coastal sediments using granulated coal ash, Mar. Poll. Bull, 83(2014)132-137.

[21] T. Yamamoto, K. Harada, K.H. Kim, S. Asaoka, I. Yoshioka, Suppression of phosphate release from coastal sediments using granulated coal ash, Estuar. Coast. Shelf Sci., 116 (2013) 41-49.

[22] K. Kido, T. Saito, R. Uotani, T. Kuwahara, M. Aizaki, Estimate of the

Efflux of N·P·S from Sediment in Dredging Hollow in Lake Nakaumi and Effect of Sand Capping with Granulated Coal Ash, J. Jpn. Soc. Water Environ. 37 (2014)71-77, Japanese with English abstract.

Figure Captions

Fig.1 Flow diagram of hydrogen sulfide removal experiments with the GCA

Fig.2 Sampling stations of field experiment sites

Fig. 3 Removal amount of hydrogen sulfide with time by the GCA at each the number of removal tests

(a) And (b) are initial concentration 10 and 100 mg-S L^{-1}, respectively.

Error bar represents standard deviation conducted in triplicates.

Fig. 4 Sulfur K edge XAFS spectra of sulfur standard and the white colored precipitation

H_2S 5th and 10th; The 5 and 10 times of hydrogen sulfide adsorption under anoxic condition, respectively. : Oxic 5st and 10th; The 5 and 10 times of regeneration under oxic condition, respectively.

Fig. 5 Manganese K edge XAFS spectra of manganese standards and the GCA from the removal experiments

H_2S 1st-10th; The number of times of hydrogen sulfide adsorption under anoxic condition. : Oxic 1st~5th; The number of times of regeneration processes under oxic condition

Fig. 6 Iron K edge XAFS spectra of the GCA from the removal experiments

H_2S 1st-10th; The number of times of hydrogen sulfide adsorption under anoxic condition. : Oxic 1st~5th; The number of times of regeneration processes under oxic condition

Fig. 7 Sulfur K edge XAFS spectra of standards and the GCA from the removal experiments

H_2S 1st-10th; The number of times of hydrogen sulfide adsorption under anoxic condition. : Oxic 1st~5th; The number of times of regeneration processes under oxic condition

Fig. 8 Manganese K edge XAFS spectra of standards and the GCA collected from the field experiment sites

Fig. 9 Positive correlation between the peak top energy of manganese XANS in the GCA and the oxidation and reduction potential of the sediments

Fig. 10 Sulfur K edge XAFS spectra of standards and the GCA collected from the field experiment sites

Fig. 11 Regeneration mechanisms of the adsorption site for hydrogen sulfide on the GCA

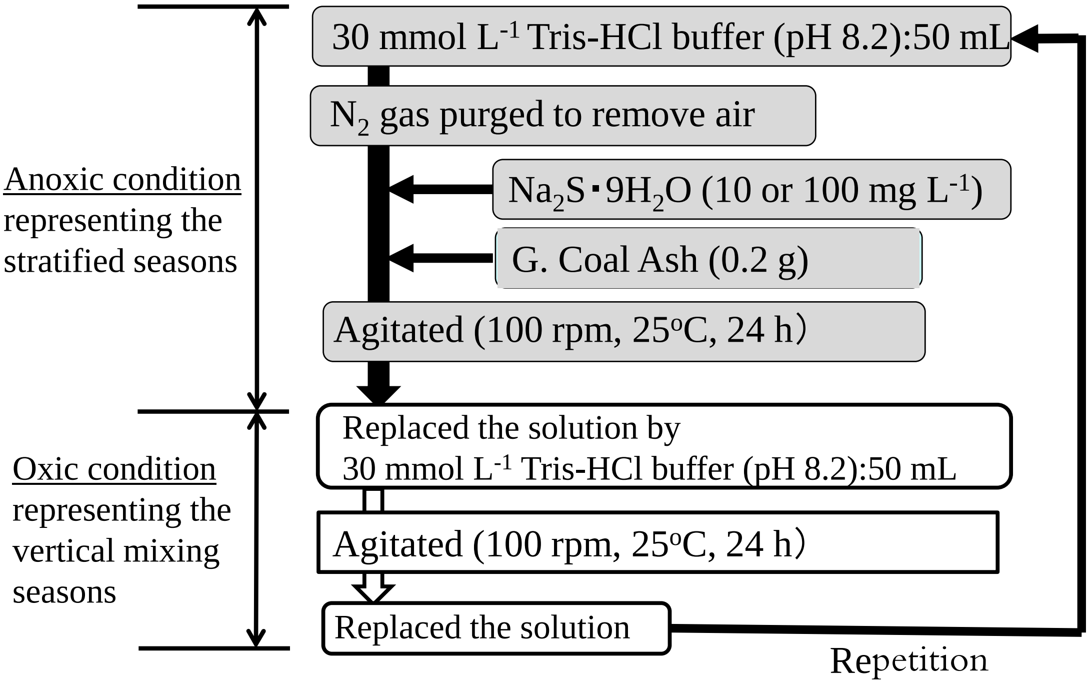
30 mmol L-1 Tris-HCl buffer (pH 8.2):50 mL
N2 gas purged to remove air
Na2S・9H2O (10 or 100 mg L-1)
G. Coal Ash (0.2 g)
Agitated (100 rpm, 25°C, 24 h)
Replaced the solution by
30 mmol L-1 Tris-HCl buffer (pH 8.2):50 mL
Agitated (100 rpm, 25°C, 24 h)
Replaced the solution
Repetition
Anoxic condition
representing the
stratified seasons
Oxic condition
representing the
vertical mixing
seasons

Fig.1

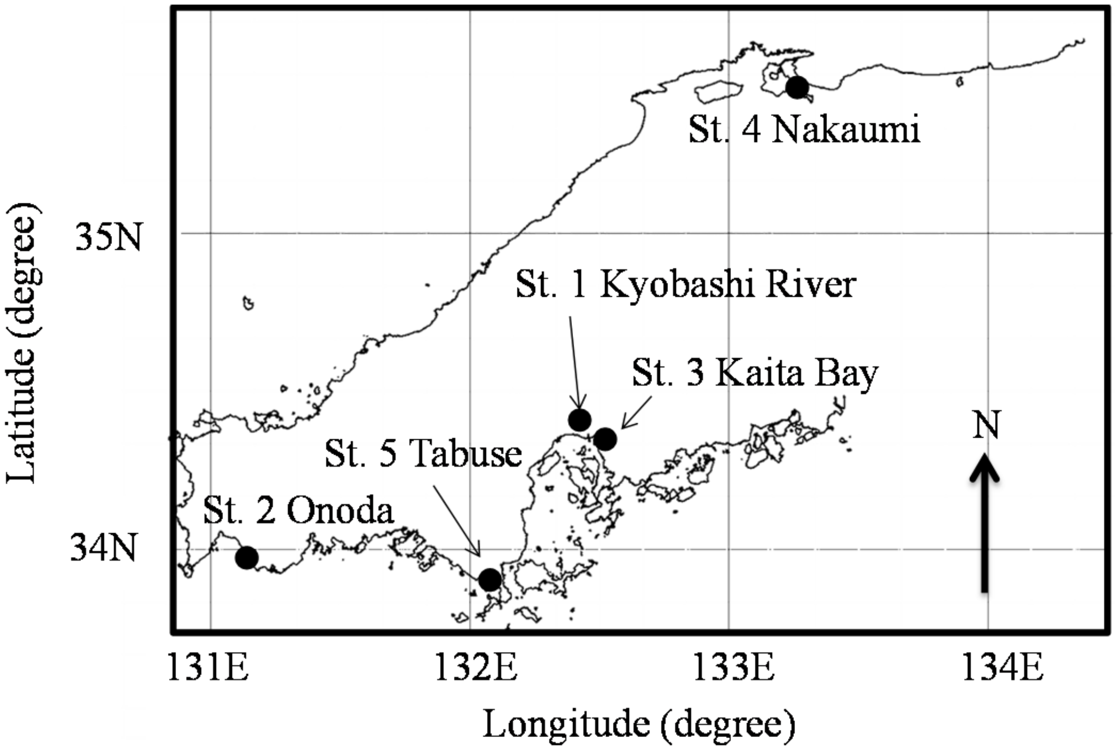
St. 4 Nakaumi
St. 1 Kyobashi River
St. 3 Kaita Bay
St. 5 Tabuse
St. 2 Onoda
N
35N
34N
131E
132E
133E
134E
Latitude (degree)
Longitude (degree)

Fig. 2

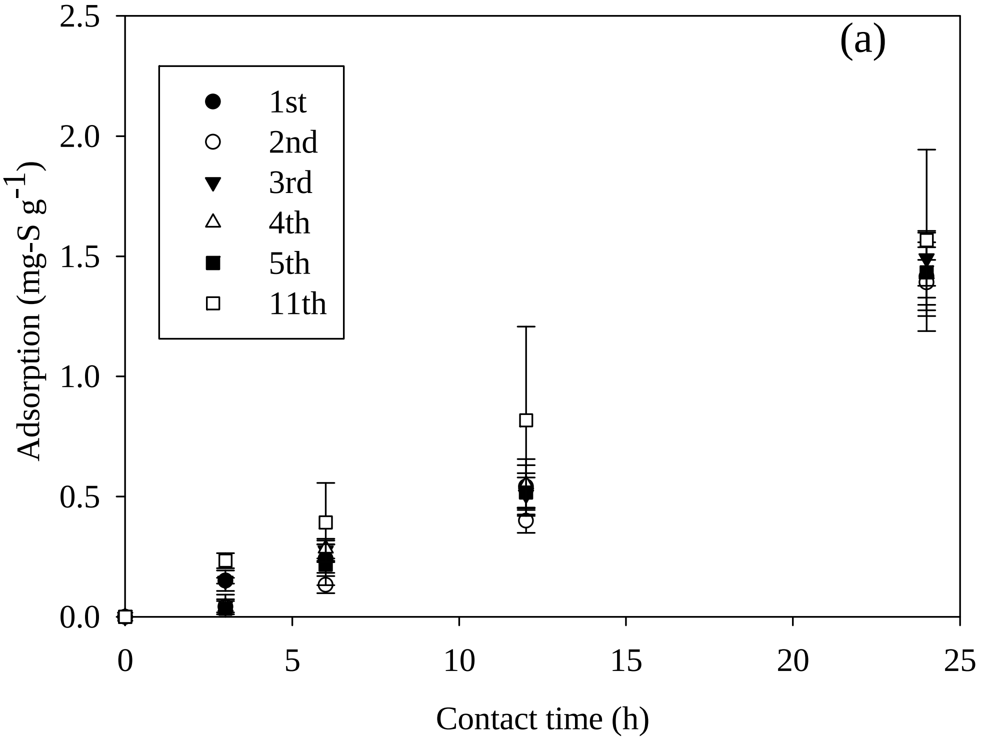
(a)
Adsorption (mg-S g^{-1})
0.0
0.5
1.0
1.5
2.0
2.5
0
5
10
15
20
25
Contact time (h)
● 1st
○ 2nd
▼ 3rd
△ 4th
■ 5th
□ 11th

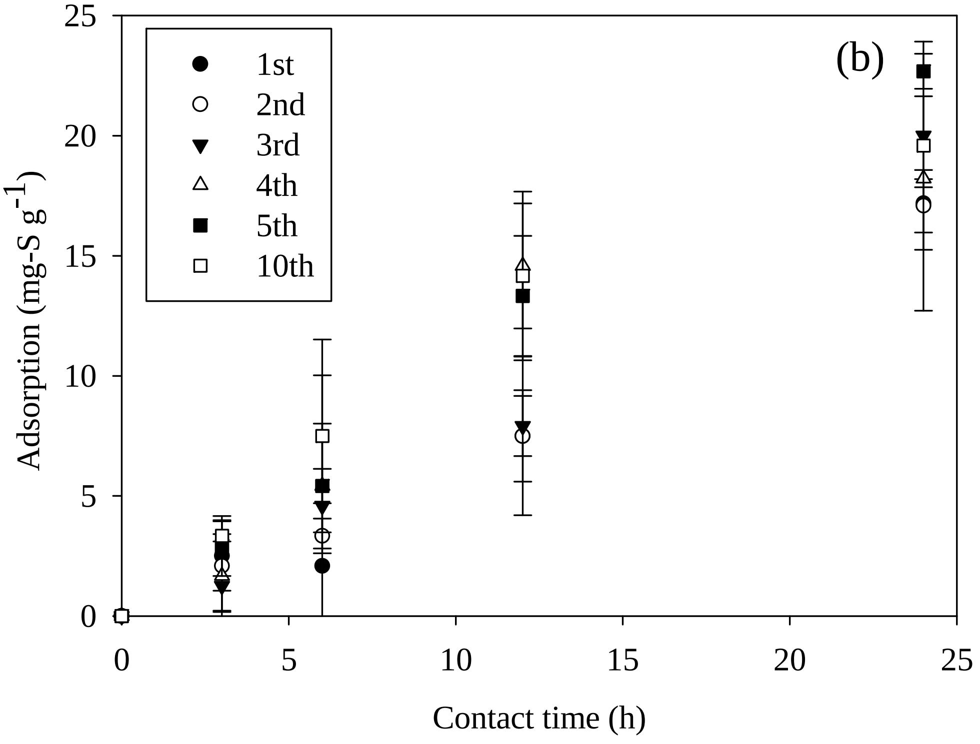
(b)
Adsorption (mg-S g^{-1})
0
5
10
15
20
25
0
5
10
15
20
25
Contact time (h)
● 1st
○ 2nd
▼ 3rd
△ 4th
■ 5th
□ 10th

Fig. 3

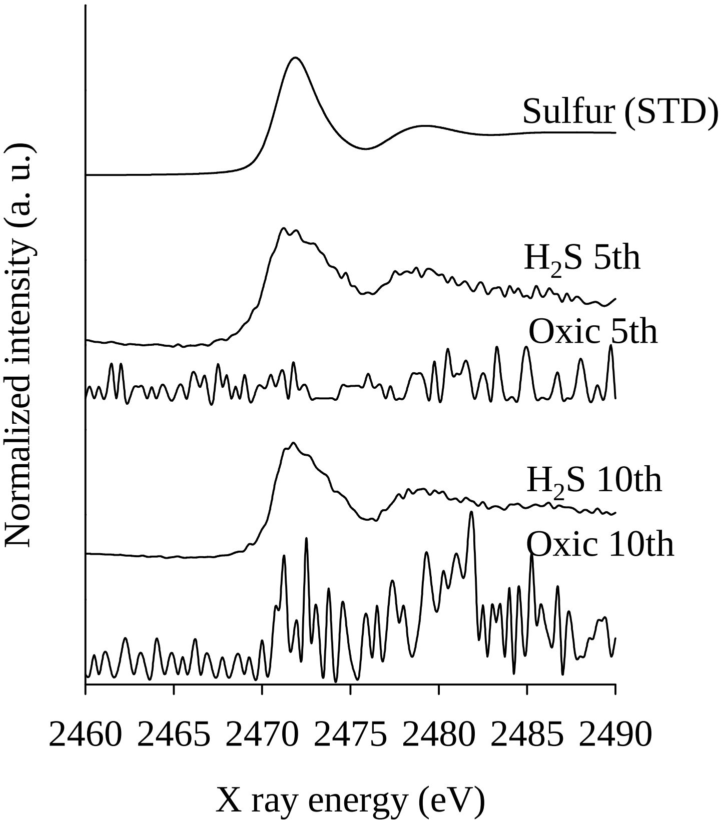
Sulfur (STD)
H2S 5th
Oxic 5th
H2S 10th
Oxic 10th
Normalized intensity (a. u.)
2460
2465
2470
2475
2480
2485
2490
X ray energy (eV)

Fig. 4

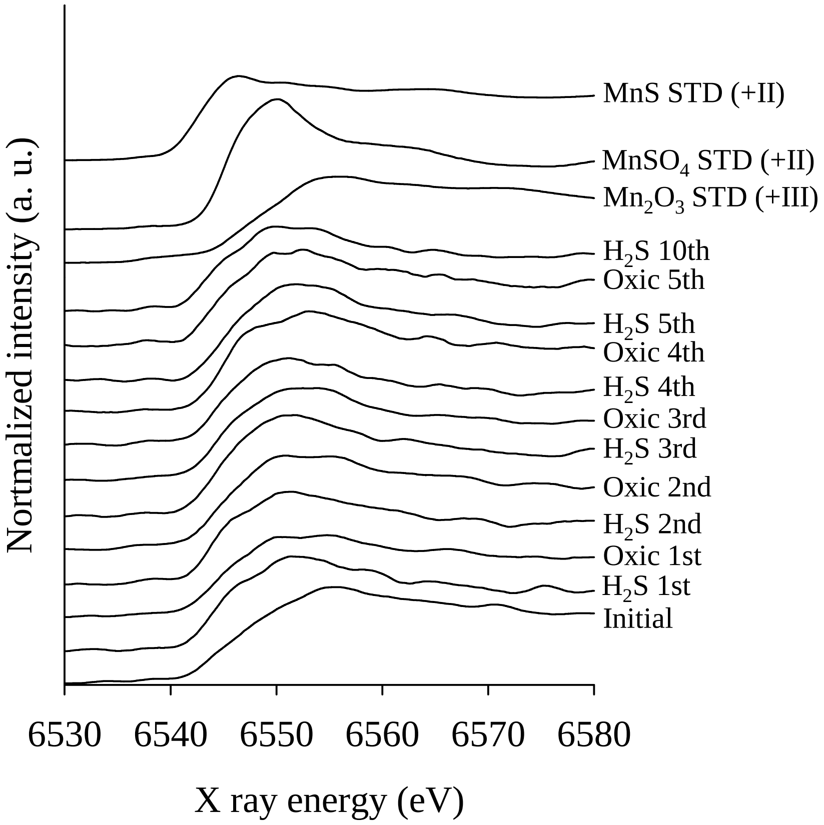
Normalized intensity (a. u.)
MnS STD (+II)
MnSO$_4$ STD (+II)
Mn$_2$O$_3$ STD (+III)
H$_2$S 10th
Oxic 5th
H$_2$S 5th
Oxic 4th
H$_2$S 4th
Oxic 3rd
H$_2$S 3rd
Oxic 2nd
H$_2$S 2nd
Oxic 1st
H$_2$S 1st
Initial
6530
6540
6550
6560
6570
6580
X ray energy (eV)

Fig. 5

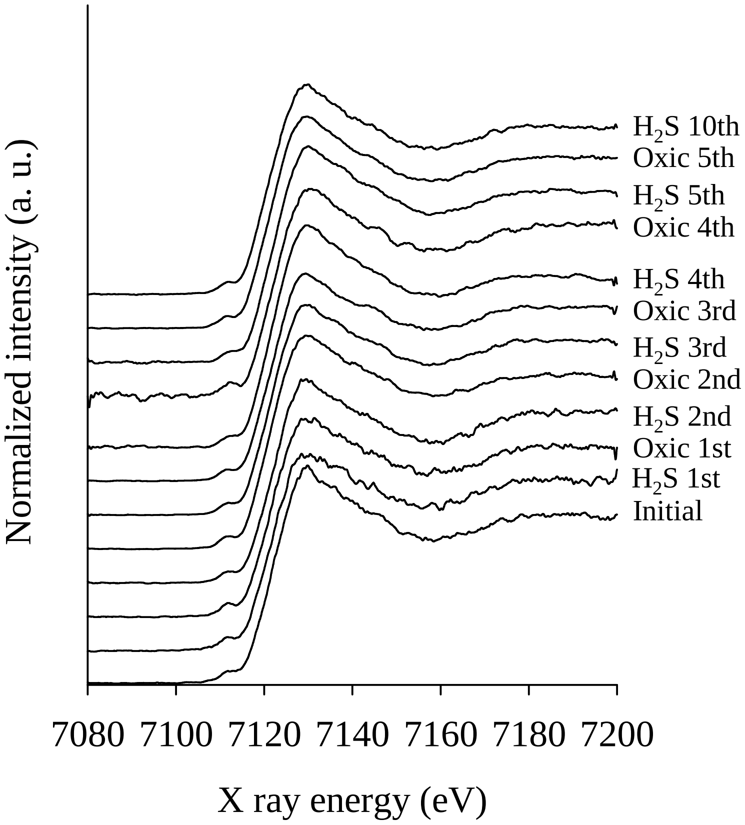
Normalized intensity (a. u.)
X ray energy (eV)
7080
7100
7120
7140
7160
7180
7200
H2S 10th
Oxic 5th
H2S 5th
Oxic 4th
H2S 4th
Oxic 3rd
H2S 3rd
Oxic 2nd
H2S 2nd
Oxic 1st
H2S 1st
Initial

Fig. 6

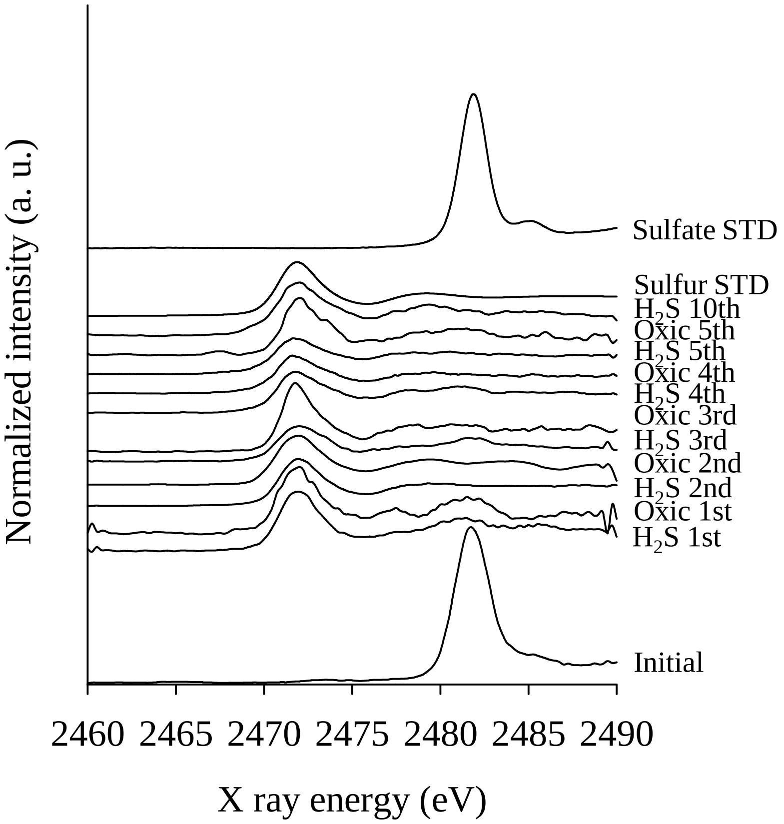
Normalized intensity (a. u.)
Sulfate STD
Sulfur STD
H2S 10th
Oxic 5th
H2S 5th
Oxic 4th
H2S 4th
Oxic 3rd
H2S 3rd
Oxic 2nd
H2S 2nd
Oxic 1st
H2S 1st
Initial
2460
2465
2470
2475
2480
2485
2490
X ray energy (eV)

Fig. 7

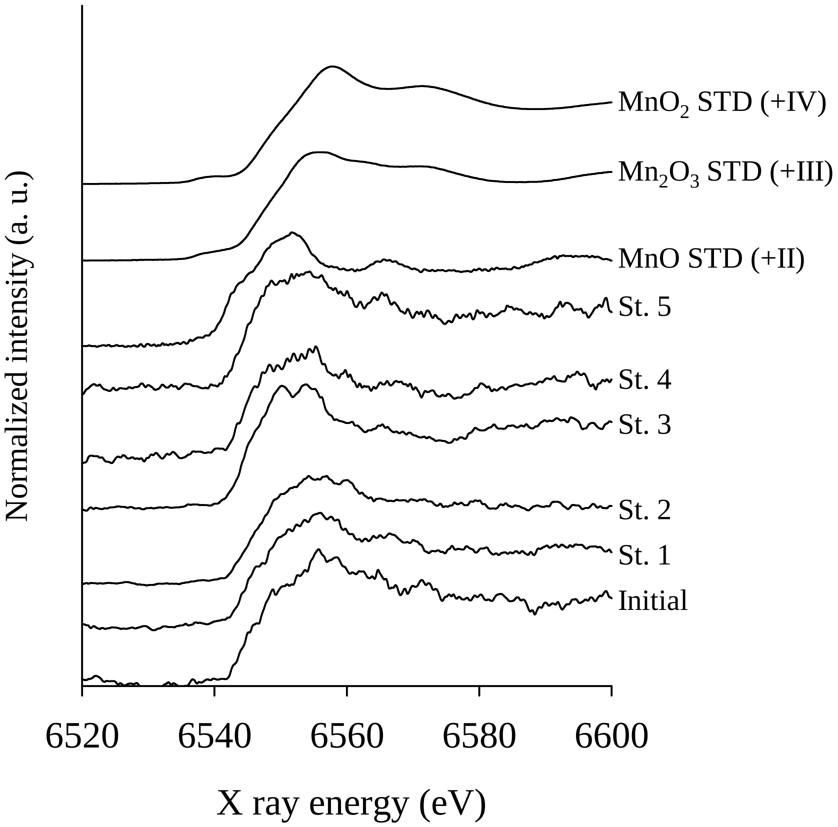
Normalized intensity (a. u.)
MnO$_2$ STD (+IV)
Mn$_2$O$_3$ STD (+III)
MnO STD (+II)
St. 5
St. 4
St. 3
St. 2
St. 1
Initial
6520
6540
6560
6580
6600
X ray energy (eV)

Fig. 8

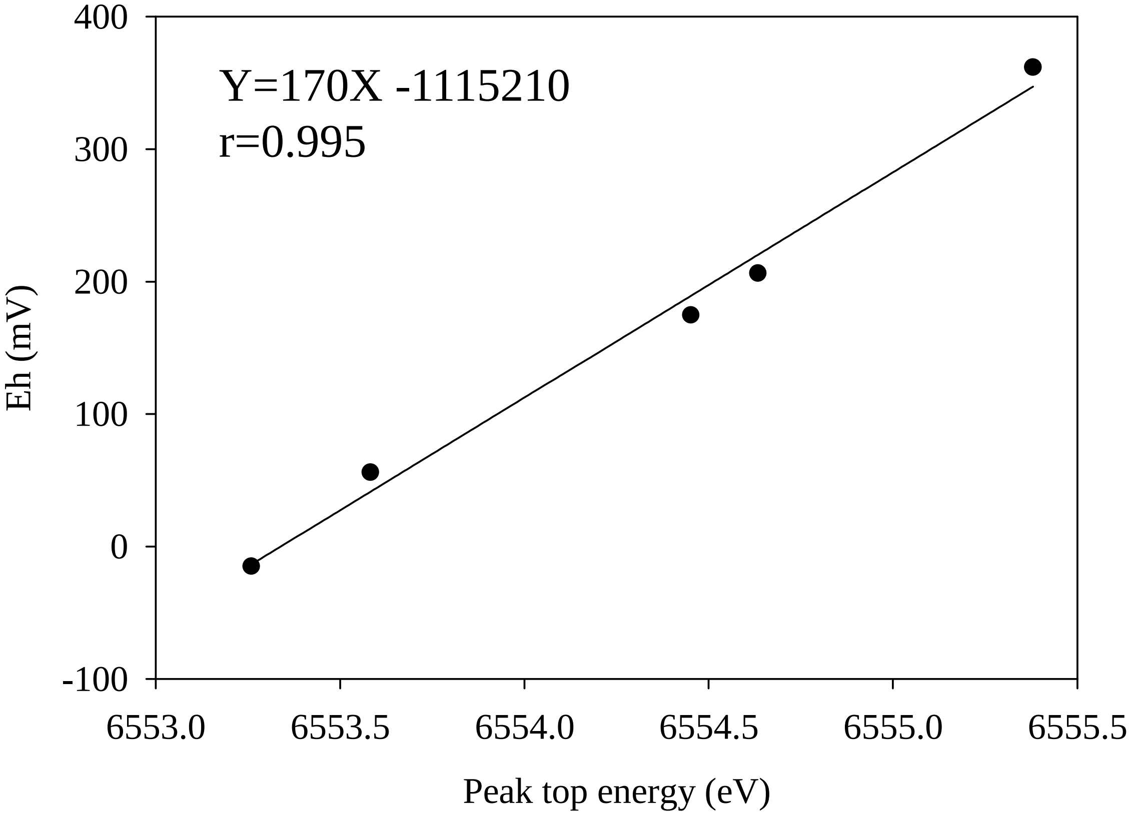
Y=170X -1115210
r=0.995
Eh (mV)
400
300
200
100
0
-100
6553.0
6553.5
6554.0
6554.5
6555.0
6555.5
Peak top energy (eV)

Fig. 9

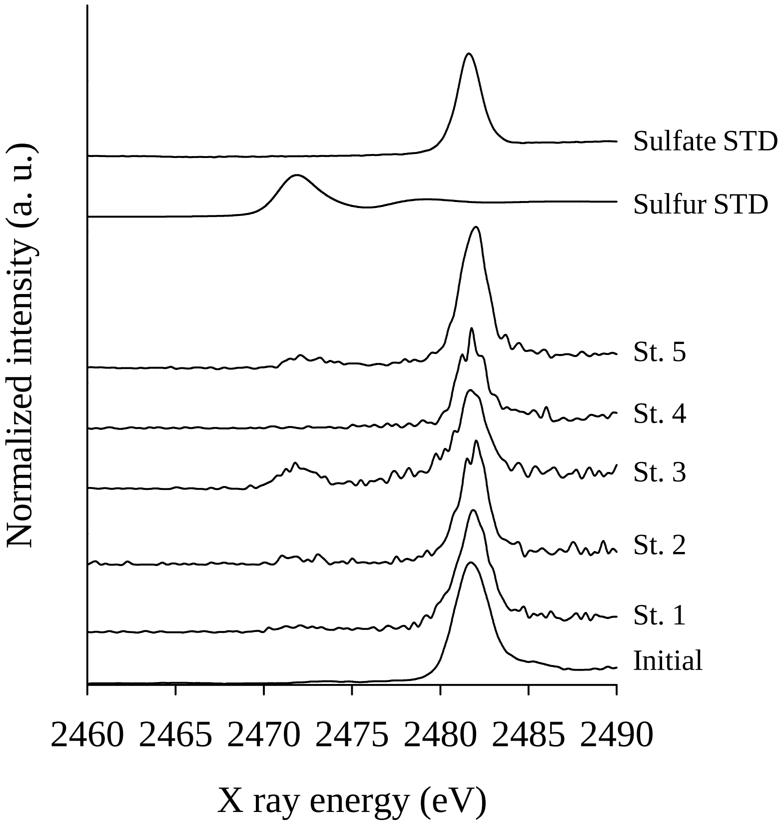
Normalized intensity (a. u.)
Sulfate STD
Sulfur STD
St. 5
St. 4
St. 3
St. 2
St. 1
Initial
2460
2465
2470
2475
2480
2485
2490
X ray energy (eV)

Fig. 10

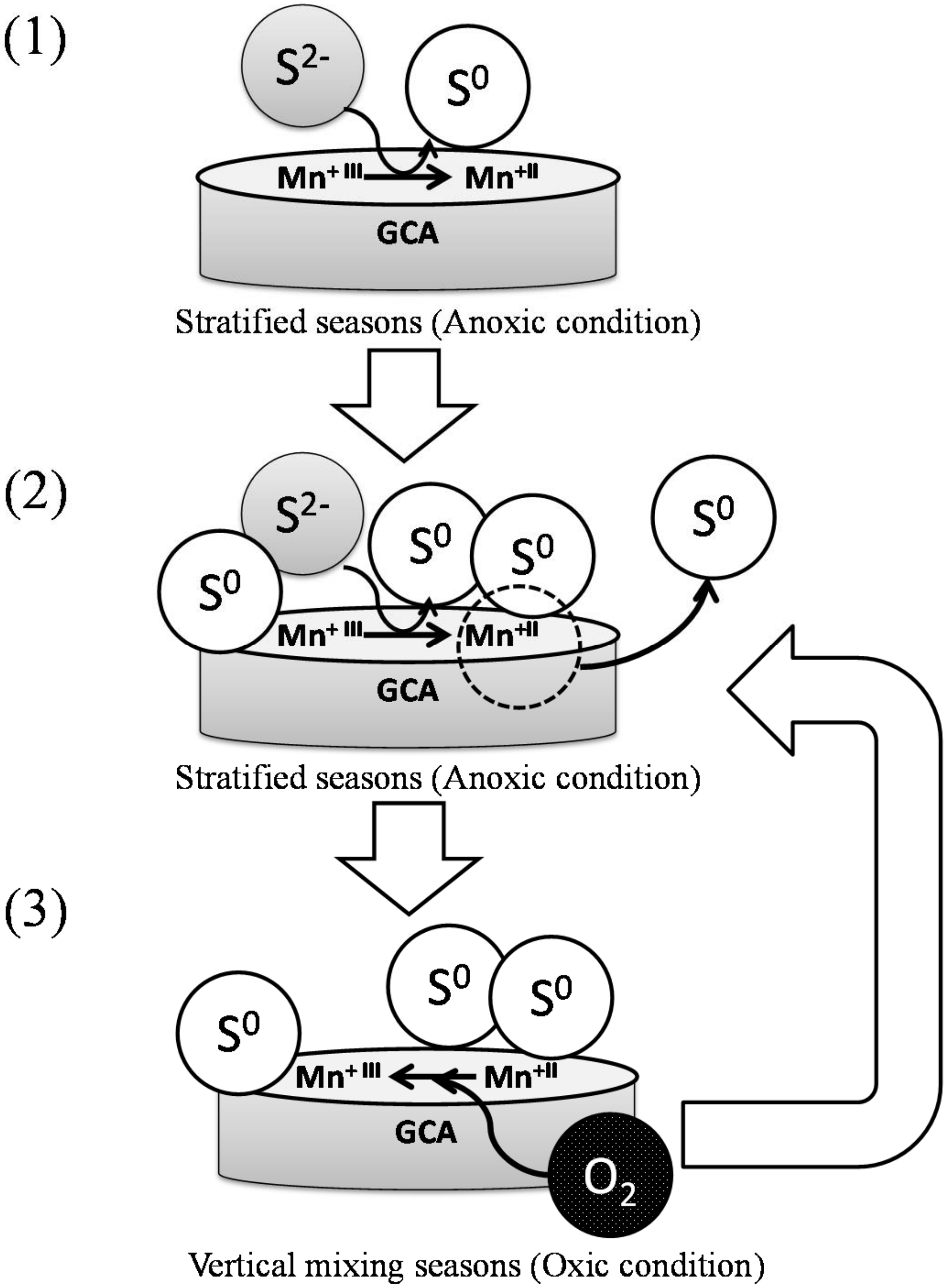
(1)
S^{2-}
S^0
Mn^{+III}
Mn^{+II}
GCA
Stratified seasons (Anoxic condition)
(2)
S^{2-}
S^0
S^0
S^0
S^0
Mn^{+III}
Mn^{+II}
GCA
Stratified seasons (Anoxic condition)
(3)
S^0
S^0
S^0
Mn^{+III}
Mn^{+II}
GCA
O_2
Vertical mixing seasons (Oxic condition)

Fig. 11

Table

Table 1 Field data of the experiment sites

St. No	St. Name	latitude	longitude	DO of overlying water(mg L^{-1})	pH of sediment	Salinity of overlying water (psu)	Eh of sediment (mV)	H_2S in pore water (mg L^{-1})
1	Kyobashi-River	N34^{o}23' 36"	E132^{o} 28' 09"	0.3	8.2	1.6	362	<0.002
2	Onoda	N33^{o}58' 12"	E131^{o} 08' 45"	6.75	7.9	Missing value	56.0	Missing value
3	Kaita Bay	N34^{o}20' 49"	E132^{o} 30' 39"	7.30	8.1	31.4	-14.9	<0.002
4	Nakaumi	N35^{o}26' 03"	E133^{o} 16' 54"	0.02	7.6	30.4	207	11.6
5	Tabuse	N33^{o}53' 39"	E132^{o} 03' 18"	6.5	7.6	32.4	175	0.29